RZ 3322 (#93368) 12/25/00
Materials Science 14 pages

Research Report

Computer Simulations for Organic Light-Emitting Diodes

Alessandro Curioni and Wanda Andreoni

IBM Research
Zurich Research Laboratory
8803 Rüschlikon
Switzerland

COMPUTER SIMULATIONS FOR ORGANIC LIGHT-EMITTING DIODES

Alessandro Curioni and Wanda Andreoni
IBM Research, Zurich Research Laboratory, 8803 Rüschlikon, Switzerland

Abstract

The physical and chemical properties of tris(8-hydroxyquinolinato)aluminum (Alq_3), one of the organic materials most commonly used as the light-emitting layer of OLEDs, and the interface with possible metal cathodes are investigated by means of first-principles computer simulations. A number of new insights have emerged from this study, and we emphasize the consequences of the properties thus discovered with respect to the functioning of the OLED device. In particular, novel Alq_3 derivatives can be designed with the aid of computations that should enhance the intrinsic luminescence of the pristine material.

1. Introduction

Organic-light-emitting devices (OLEDs) represent a promising solution for the flat panel displays of the new generation. The key element of these multicomponent systems is the organic compound used as a light emitter. OLEDs based on polymers have poly-paraphenylene-vinylene (PPV) as the prototype but during the years a number of derivatives of PPV or other polymers have been proposed and used OLEDs based on "small molecules", on the contrary, have tris(8-hydroxyquinolinato)aluminum (Alq_3) as the prototype and only a few derivatives have been proposed so far. In all cases, it becomes clearer with time that, in order to make progress in the improvement of device characteristics, a deeper understanding is needed at the microscopic level. In this effort, computer simulations can be of substantial help and can efficiently complement experimental information, provided they rely on accurate models and methods. Our own calculations, which are based on the state-of-the-art methods of computational chemistry, have been focused on Alq_3-based OLEDs, and in particular on the study of Alq_3 and its interaction with the metals typically used as cathodes. The results of this work are aimed at gaining insight into fundamental issues such as the mechanisms of charge injection and transport, the processes responsible for electroluminescence as well as degradation, and also at providing a guide to the optimization and development of novel materials.

In this paper we report briefly on our published work [1-4], and present new results on the optical spectrum of Alq_3 and on the electronic properties of the solid phase. We also introduce additional findings for complexes having metal atoms, and finally propose new Alq_3 derivatives having a higher intrinsic luminescence.

2. Method

Our calculations are parameter-free and use current implementations of density-functional theory (DFT) [5] with gradient-corrected exchange and correlation functionals, according to Becke [6] and Lee, Yang, and Parr [7]. The basis set for the expansion of the electronic wave functions consists of plane waves, while the core–valence interaction is represented by norm-conserving angular-momentum-dependent pseudopotentials. All computational details are given in Reference [1]. The types of calculations [8] that we have performed on these materials are diverse:

i) Structural optimization of the organic molecules, which may be isolated, part of crystal structures, or deposited on a metal surface.
ii) Identification of the chemical properties of the above systems, namely their bonding and their response to the addition of charges and to the interaction with foreign atoms and ions.
iii) Determination of features of the electronic structure that are directly comparable to data from photo-emission, near-edge X-ray absorption fine structure (NEXAFS) and optical absorption.
iv) Calculation of their vibrational properties, with frequencies and intensities directly comparable to infrared (IR) and Raman spectra.
v) Car–Parrinello (CP) molecular dynamics (MD) [9] simulations of the organic/metal interfaces at constant temperature, which are useful in monitoring the time evolution of interacting systems at several different levels of coverage and the effect of different temperature conditions.

3. The organic material: Alq_3

3.1. Molecular isomers: structural and electronic properties

Alq_3, is a tris-chelate organometallic complex in which the metal atom (Al) has a distorted octahedral coordination. It can exist in either of the two geometrical isomers shown in Figure 1: the "meridianal" (C_1 symmetry) isomer or the "facial" (C_3 symmetry) isomer, which differ in the relative position of the oxygens and nitrogens of the metal coordination shell. Both geometrical isomers are chiral and thus correspond to two different optical isomers. As suggested in Reference 1, this property can be exploited to obtain an organic material with interesting optical properties.

All details of the optimized structural characteristics, of the energetics, and of the electronic properties are reported in Reference [1]. The results are briefly summarized below.

The meridianal isomer is lower in energy by ~4 kcal/mol while the facial isomer has a larger dipole moment. Although the crystal phases characterized so far [10] show only the presence of the meridianal isomer, it is not possible on the basis of the theoretical results alone to make predictions about the relative stability of the two isomers in condensed phases. In fact, not only may intermolecular interactions affect the energetics, but different molecular conformations can have different preferential packing. As already argued [11] and now confirmed by our results, the two isomers may well coexist in the amorphous phase. Moreover, such a

coexistence can be seen as a factor favoring the stability of the non-crystalline state itself, which appears to be a prerequisite for good performance and thermal stability of the device.

The structural difference between the two isomers does not affect the metal–chelate bonding, which is mostly ionic, with aluminum transferring almost three electrons to the oxygen atoms. We have not yet been able to identify an experiment that can easily detect either isomer. In fact, our calculations of the electron densities of states (DOS) show negligible differences between the two isomers, so that for example photoemission does not appear to be useful for this purpose. Infrared (IR) and Raman spectra are expected to be more sensitive to molecular geometry. However our calculations show that in the case of Alq_3, they are unable to distinguish between the two isomers because the activity of the vibrational modes that distinguish them is too low.[1]

Given the quasi-equivalence of the three ligands, the sequence of one-electron energy levels in a Kohn-Sham diagram [5] can be described as a series of "triplets" whose splitting differs in the two different structures.

To validate the calculated electronic structure, we have compared it in Reference [2] to experiments on amorphous films. The density of the occupied valence states (DOS) was compared with photoemission (PES) data (see Figure 2) and the photoabsorption function from the 1s core states for C, N, and O with NEXAFS data (see Figure 3). Interestingly, both calculated spectra can be resolved into the contributions from the individual atoms or ligands or bonds: The atom-resolved DOS images the occupied electron states, yielding information on the nature of injected holes, while the photoabsorption function probes empty electron states, providing information on the nature of the injected electrons. Thus, the character of the low-energy excitations responsible for the luminescence properties of the material emerges from these calculations. Combined with experimental data gathered over time, computed spectra may provide a reference for monitoring the behavior and possible degradation of the organic material in the device.

Additional information derived from our calculations provides insight into the interrelationship of structure and electronic behavior, in particular the response of the molecule to the formation of a hole or the addition of an electron. Table 1 contains the ionization potentials (IPs), electron affinities (EAs), and extraction potentials (HEP and EEP for the hole and the electron, respectively) that refer to the geometry of the ions. Relatively small energy changes are associated with structural relaxation, and all energies reported are rather insensitive to the specific isomer. In all cases, the energy required to create a hole is ~6 eV, while the extraction of an electron from the anion requires ~1 eV. Experimental values invariably refer to the solid state. For the IP, the measured values are in the range 5.6–6.0 eV (see, e.g., [13–15]). On the other hand, the electron affinity (the binding energy of the injected electron) cannot easily be obtained experimentally. In particular, we note that previous attempts to estimate it from optical data (see, e.g., Ref. 14) are invalidated owing to the presence of strong excitonic effects.

The same calculations are also used to estimate self-trapping energies of positive and negative charges in the material. Indeed, in Ref. [11], the traps that characterize the electron transport in the material were identified as the states in which the injected electron is self-trapped in the individual molecules as a consequence of structural relaxation. The trapping energy was calculated as the difference between the lowest excited state of the neutral system in the ground-state structure and in that of the anion. The resulting value of 0.21 eV was compared with the trap energy of 0.15 eV deduced from the current–voltage characteristics. Such a procedure, however, provides an estimate of the exciton trap energy rather than that of the injected electron. Following the same interpretation for the trap states, the correct energy in our scheme is the energy gain of the excess electron due to structural relaxation, i.e., the difference EA(a)–EA(v), which we also report in Table 1, as the "small-polaron" stabilization energy (SPE) for the electron. Our value of 0.13 eV is close to the experimental estimate, and, more interestingly, the facial isomer appears to trap the electron more efficiently. This suggests that in the amorphous material, where the two isomers are expected to coexist, the minority geometrical isomers could act as the electron traps.

3.2. Solid Alq_3

A preliminary search for the preferential crystal packing has been performed for both isomers of Alq_3 using well-established classical force fields [16]. This has resulted in a number of different polymorphs that are nearly isoenergetic. This suggests another legitimate question: How and to what extent does molecular packing affect the electronic, optical, and transport properties?

As mentioned above, Alq_3 thin films are amorphous in the actual device. Their morphology is indeed quite complex, and recent experimental studies have provided evidence of the presence of different phases that are not well-identified [17]. Structural investigations have been performed on ordered solids. For quite some time, only two reports of the crystal structure of Alq_3 were available in the literature [10] and in both cases the solvent was not removed. For both crystals the unit cell is monoclinic and contains four molecular units having meridianal structure (Figure 4). Very recently, data have been published for three different crystal phases [18]

[1] Material from Ref. 12.

that are free of solvent. Two of them contain only the meridianal isomer, with different relative orientations, and the third is not well identified. In addition, the optical absorption and luminescence have been measured [18] for the first two phases, but the relative differences are small. The difference with respect to the amorphous phase is slightly more pronounced.

We have reoptimized the molecular geometry of the crystal discussed in Ref. 10. Comparison with the isolated molecule shows that solid-state effects on the structure are small, e.g., bond lengths vary by less than 0.03 Å. Both valence and conduction bands (shown in Figure 5 along some relevant directions) are characterized by low dispersion. The crystal field splits the highest occupied molecular orbital (HOMO), the lowest unoccupied molecular orbital (LUMO), and the LUMO+1 "triplets" further, so that the overall width is 0.1–0.2 eV larger than in the isolated molecule itself (~0.3 eV) [1]. The global picture we obtain[2] supports the validity of molecular calculations as representative of the fundamental electronic and optical properties of the Alq_3 material. Although interesting, the study of these properties as a function of crystalline packing yields only minimal additional understanding of Alq_3 thin films.

Both the hole and the electron effective mass tensors were calculated at specific k-points, and turned out to be strongly anisotropic. This suggests that the hole as well as the electron mobility may vary significantly depending on the specific molecular packing.

In conclusion, we emphasize that the band model must be regarded more as a reference than as a close approximation of the real system, even in the crystal phase. In fact, as we have seen above, the stabilization energy of the "small-electron polaron" that we have calculated for the meridianal isomer is ~0.06 eV, namely of the order of the width of the relevant energy bands. This indicates a strong electron-phonon coupling, which compromises the validity of the electronic band picture.

3.3. Optical properties

Simulating the optical excitation spectrum of Alq_3 using a reliable method is crucial for the understanding of the mechanisms responsible for photoabsorption and photoemission. As demonstrated above, the DFT-Kohn–Sham (KS) scheme for the one-electron states can be used to obtain a meaningful description of the orbital nature of the electronic structure [2]. However, the orbital energies have no direct physical meaning and, in particular, are not the quasi-particle energies. In particular, the HOMO–LUMO gaps are known to underestimate the first excitation energy gap. Thus, the usefulness of absorption spectra derived from such calculations is limited.

In our particular case, we estimated the lowest excitation energy using a modified Slater transition-state method [20] . The correction to the KS gap thus obtained was applied as a rigid shift to the remainder of the absorption spectrum. Note that this correction also contains to some extent the effect of the electron–hole interaction (excitonic effect). The spectral intensities were simply evaluated using the KS description of the hole and electron states involved in the optical excitations, neglecting the effects of the electron–hole interaction. Although electron-hole interactions are expected to alter the peak intensities, they are not expected to play a role in determining the nature of the lowest energy excitation — our main issue of concern, which we explain below.

The coupling of the hole and the electron states involved in the optical excitations is mainly dependent on their relative spatial localization. Figure 6 show the distribution of three orbital "triplets": the HOMO (0), the LUMO (I), and the LUMO+1 (II) for both isomers. The HOMOs are localized mainly on the phenoxide moiety of the ligands, while the LUMOs localize mainly on the pyridyl moiety. The LUMO+1 orbitals (II) are more uniformly distributed on the sides of the ligands. Owing to this type of electron distribution, the dipole transitions from the HOMOs (0) to the LUMOs (I) have weak matrix elements in both isomers, whereas the LUMO+1s (II) strongly couple to both sets. Therefore, the strongest optical absorption corresponds to transitions from (0) to (II), not from (0) to (I) (at about 400 nm), i.e., between the states responsible also for the photoemission [(I) to (0)]. Note that the latter involve energy gaps that are about 1 eV higher. This is shown in Figure 7, where the calculated absorption spectrum of the meridianal molecular isomer of Alq_3 is reported and compared to the experimental one[3] measured for a thin Alq_3 film deposited on sapphire. Clearly, there are discrepancies in the intensities, especially at higher energies, which can be attributed to several factors, including the lack of excitonic effects in the calculated intensities and differences between calculations on an isolated molecule and measurements performed on an amorphous film.

3.4. Novel Alq_3 derivatives with enhanced performance

The result discussed above provides a clue for screening of alternative compounds based on Alq_3 derived with the purpose of obtaining more efficient organic emitters [22]. In fact, one way to increase the intrinsic

[2] Material from Ref. 19
[3] Material from Ref. 21

luminescence yield is to attempt to modify the localization of the electron states involved in the luminescence process. This can be achieved by specific chemical substitutions on the quinolate rings. The reasoning underlying such substitutions is the following: Electron-donor substituents generally destabilize the π electronic states of aromatic systems, and this effect decreases with increasing distance from the substituents. On the other hand, electron-acceptor substituents stabilize the π electronic states of aromatic systems; this effect also decreases with increasing distance from the substituting group. Therefore, a substitution on the phenoxide ring will act mainly on the HOMO set, whereas a substitution on the pyridyl ring will act mainly on the LUMO set. As the electronic states at a higher energy than the LUMOs and those at a lower energy of the HOMOs are delocalized on both rings of the quinolate ligands, the optimum substitution strategy is to put an electron-acceptor group on the phenoxide ring (enhancing the mixing of the HOMOs with the states at lower energy) and/or an electron-donor group on the pyridyl ring (enhancing the mixing of the LUMOs with states at higher energy). Moreover, owing to both electronic and structural factors, the most suitable positions for the chemical substitution are positions 4 and 5 on the quinolate ligand, namely, those "para" to the oxygen atom and the nitrogen atom (see Figure 8). This approach generated a new family of Alq_3 derivatives which were then screened by comparing the calculated absorption spectra with that of the pristine Alq_3 molecule. Of the substituent patterns we have considered, the one with R = $–CF=CF_2$ and R' = –O–R was shown by calculation to perform best, i.e., the transition probability was found to improve by a factor of 4 (see Figure 9). These computer-designed molecules are now awaiting only their chemical synthesis and experimental tests.

Moreover, the same procedure can be used to selectively modify the energy position of the HOMO (hole-acceptor state) and LUMO (electron-acceptor state), allowing the design of Alq_3 derivatives with a tuned energy gap (and hence emission wavelength) and also with optimum electron- and hole-injecting barriers.

4. Metal–organic interaction

4.1. Metal–Alq_3 interfaces

The important role played by the specific cathode/organic interface in the functioning of an OLED has emerged over the years. The insight gained so far into the mechanisms leading to a certain degree of performance is, however, still rudimental, rendering control and optimization a very difficult task. An attempt is made in these calculations to provide enhanced insight through calculations.

As a model for these interfaces, we consider two-dimensional (2D) periodic slabs of metal atoms consisting of a few layers, separated by a vacuum region of similar thickness and having one Alq_3 on top. As metals, we consider lithium, aluminum, and calcium. On the basis of work-function values only (2.38 eV for Li; 4.25 eV for Al; 2.80 for Ca), lithium would be the most desirable as an electron-injecting material. In practice, however, lithium cannot be used as a contact metal because it causes the organic ligands to degrade within seconds (see e.g. [23]). On the contrary, aluminum metal and its alloys with lithium, or calcium are used as typical cathodes in OLEDs.

The computational approach we have followed consisted of a number of CP-MD simulations performed at room temperature. Since the duration of these runs is only a few ps and thus does not allow a sufficiently large configurational space to be explored, we tried to partially overcome this limitation by using several significantly different starting configurations: namely a number of different molecular conformations for either the meridianal or the facial isomer with different orientations positioned at various distances from the surface. In this way, the behavior of these systems, which are dramatically different in the three cases, could be characterized. Representative snapshots of the MD simulations are shown in Figure 10.

In the CP-MD simulations, we can observe that lithium [Figure 10(a)] reacts with the Alq_3 moiety very rapidly, readily forming bonds with both the carbon and the oxygen atoms. In this way, the molecule loses its characteristic electronic properties. Moreover, the cathode appears to be highly unstable, and lithium atoms exhibit a strong tendency to diffuse. These findings are in agreement with the experimental observation of instability of the lithium cathode and rapid degradation of the organic material [23].

The situation is very different in the case of aluminum as can be seen in Figure 10(b) for comparable time intervals in which no formation of new chemical bonds is observed at the interface. This type of bonding, implying the absence of charge transfer, is only perturbative and can be described as physisorptive. The molecule was observed to flatten as a consequence of the interaction, and thus preserves all its electronic characteristics. This is shown by the DOS in Figure 11(a) that refers to the occupied states. Owing to the dominant Al character near the Fermi energy, the nature of the corresponding states cannot be ascertained from either the total DOS or an experimental spectrum, but the projection of the DOS on the molecular orbitals can elucidate this point.

Calcium [Figure 10(c)] behaves in an intermediate way: Alq_3 is strongly chemisorbed on the surface, owing mainly to the formation of new covalent bonds between the surface and the Alq_3 oxygen atoms. A sizable

charge transfer from the metal surface to the Alq_3 LUMOs takes place, as can be seen from the DOS in Figure 11(b). The additional peak at the Fermi energy corresponds well to the LUMO of the molecule. Therefore, in contrast to aluminum, calcium has an intrinsic tendency to transfer electrons to the organic material. We have also studied Li_nAl layers in interaction with Alq_3 and have found that one Al layer is very efficient in blocking metal diffusion into the organic layer owing to the strong Li–Al attractive interaction. Also, such a system could be more efficient than aluminum as electron-injecting material because the work function is lowered by the transfer of electrons from lithium to the aluminum layer [23].

Our simulations clearly show that the nature of the Alq_3–cathode interaction depends critically on the metal used for the latter and that this interaction can strongly perturb the geometrical as well as the electronic structure of the Alq_3 molecule. Therefore the use of non-atomistic, oversimplified models for the study of these interfaces is questionable (see, e.g., [24]). In fact, these methods rather simplistically assume that only charge transfer and a shift of the HOMO and/or LUMO levels occur, whereas in reality even a radical change of the nature of the frontier orbitals can take place. Indeed, our findings for the aluminum and calcium interfaces are fully consistent with recent internal photoemission data [25] which clearly indicate that they behave differently, namely, that the Schottky energy barrier cannot be deduced from the same type of model.

4.2. Metal–Alq_3 complexes

Complexes with single metal atoms are expected to form in metal-doped Alq_3 layers and at a cathode–organic interface in the early stages of metal deposition or during degradation processes. Although their presence has often been invoked to interpret experimental observation, characterization by experiment has not been possible. Reliable modeling and accurate calculations can provide such a characterization and can also determine the effects that the formation of such complexes may have on the intrinsic properties of the organic material. This was the motivation of our extended study [3], which was based on a thorough structural optimization of complexes of individual metal atoms of Li, Al, and Ca with both geometrical isomers of Alq_3. Here we give only a brief summary of the main results.

It was established that two important features of the interaction of the organic with the metal atom are independent of whether it is Li, Al, or Ca:

i) The Alq_3 oxygen atoms are the centers of attraction of any "electron donor," so that complexes with the metal close to them are strongly favored energetically. This is clear from Figure 12, which shows the optimum configuration for the three complexes in both isomers.

ii) As can be seen in Table 2, all of these complexes are strongly bound, and much more so with the molecule in the facial configuration (~10–15 kcal/mol more). Therefore, the interaction with the metal atom inverts the relative stability of the two isomers of pure Alq_3 (see the subsection on molecular isomers in Section 3), and the energy difference becomes large. We believe that, given the significantly different abilities of the two isomers to trap an electron, such an inversion of stability should not be overlooked when electron-injection or electron-transport processes are discussed.

Other important features, such as the type of chemical bonding which influence the modification of the Alq_3 electronic structure induced are more specific to the type of metal used.

Simple criteria such as that based on the Mulliken electronegativity would predict a higher tendency for an electron to escape from the metal atom to the molecule than vice versa in all cases, mainly because of the higher electron affinity of the latter [~1 eV vs. 0.6 (Li) , 0.4 (Al), and 0.02 eV (Ca)]. Indeed, the π system of the Alq_3 molecule accepts one electron from the atoms. However, the transfer can be considered almost complete only in the case of Li, and the degree of hybridization (or the degree of bond covalency) can be seen to increase in the sequence Li, Al, Ca. As a consequence, a parallel increase the activation energy can be predicted for the diffusion of the metal atom into the organic layers.

As mentioned above, the formation of these complexes is often argued in connection with unclear experimental data. In particular, complexes are supposed to play a role in the quenching of luminescence by the creation of new levels in the gap of the organic. Although our results indicate that this is always the case, the mechanisms will be different because the origin of the "additional level" is different in the three cases: In Li:Alq_3, it corresponds to the LUMO of the organic ligands, in Ca:Alq_3 to a (doubly occupied) state resulting from the strong hybridization of the LUMO with the 4*s* Ca orbital; and in Al:Alq_3 to the Alq_3 HOMO that is destabilized by the interaction with the Al 3*s* orbital.

Table 3 shows the values of the ionization potentials, electron affinities and self-trapping ("small polaron") energies for these three complexes, evaluated for the facial isomer, which can be directly compared with corresponding values for the isolated molecule in Table 1. The most interesting message is that the self-trapping energy for an electron is very strongly reduced because of the increased structural rigidity induced by the interaction with the metal atom.

5. Summary and Conclusions

OLEDs are a relatively new type of device. Because of this, the fundamental science underlying their functioning is still largely unexplored or poorly understood, and this may ultimately constitute an inhibiting factor for progress in the development of better performing materials. Computer simulations may play an important role for the characterization of materials behavior at a microscopic level, provided a certain level of reliability of the modeling and theoretical approach is guaranteed. In this paper, we have discussed our own contribution in this effort, using *ab-initio* calculations of Alq_3 in the molecular state, in the crystal phase and deposited on metal surfaces simulating the electron injecting material. The knowledge of electronic, structural, vibrational and optical properties that we have gained through these calculations, and of the chemistry of the interfaces with the cathode, allow us to progress slowly toward our goal of suggesting how to improve the performance of the multicomponent system. We have succeeded in identifying the crucial electronic factors that limit the intrinsic luminescence of Alq_3 and have made precise suggestions for improving it by making specific substitutions on the ligands. Optimizing the characteristics of the interface of Alq_3 with the cathode is also an important task, which now requires more systematic computational work. Simulations on clean surfaces are the basis for understanding the intrinsic properties of the interfaces and thus developing a correct picture of the interaction. The type of simulations we have been carrying out can be naturally extended to more structurally complex cases, in which an insulating layer is interposed between Alq_3 and the metal. In fact, there is a clear need for insight to be gained into the mechanism(s) through which the addition of such a component into the device (typically LiF) lowers the electron injection threshold and thus improves the device performance. *Ab-initio* molecular dynamics can also provide a substantial contribution to the study of degradation processes whose origin and development are frequent issues of debate.
In conclusion, we believe that computer simulations of the type we have presented here have a strong potential, given their ability to detect and unravel phenomena at the microscopic level in a more direct way than experiments. However, it must be emphasized that such an approach risks remaining sterile if it is not constantly supported and stimulated by data exchange and feedback from experiment.

6. References and notes

1. A. Curioni, M. Boero, and W. Andreoni, "Alq_3: Ab initio Calculations of Its Structural and Electronic Properties in Neutral and Charged States," *Chem. Phys. Lett*. **294**, 263-271 (1998).
2. A. Curioni, W. Andreoni, R. Treusch, F. J. Himpsel, E. Haskal, P. Seidler, C. Heske, S. Kakar, T. van Buuren, and L. J. Terminello, "Atom-Resolved Electronic Spectra for Alq_3 from Theory and Experiment," *Appl. Phys. Lett*. **72**, 1575-1577 (1998).
3. A. Curioni and W. Andreoni, "Metal–Alq_3 Complexes: The Nature of the Chemical Bonding," *J. Am. Chem. Soc.* **121**, 8216-8220 (1999).
4. A. Curioni and W. Andreoni, "The Organic–Cathode Interface in Alq_3-Based Organic Light-Emitting Devices: New Insights from ab-initio Molecular Dynamics," *Synth. Met.* **111-112,** 299-301 (2000).
5. P. Hohenberg and W. Kohn, "Inhomogeneous Electron Gas," *Phys. Rev*. **136**, B864-B887 (1964); W. Kohn and L. J. Sham, "Self-consistent Equations Including Exchange and Correlation Effects," Phys. *Rev.* **140**, A1133-A1138 (1965); R. G. Parr and W. Yang, *Density Functional Theory of Atoms and Molecules*, Oxford Science Publications, New York, 1989; R. M. Dreizler and E. K. U. Gross, *Density Functional Theory*, Springer, Berlin, 1990.
6. A. D. Becke, "Density-Functional Exchange-Energy Approximation with Correct Asymptotic Behavior," *Phys. Rev. A* **38**, 3098-3100 (1998).
7. C. Lee, W. Yang, and R. G. Parr, "Development of the Colle-Salvetti Correlation-Energy Formula into a Functional of the Electron Density," *Phys. Rev. B* **37**, 785-789 (1988).
8. All calculations used the CPMD code in the parallel 2.5 version (© IBM Corp.) developed by J. Hutter.
9. R. Car and M. Parrinello,"Unified Approach for Molecular Dynamics and Density-Functional Theory,"*Phys. Rev. Lett.* **55,** 2471-2474 (1985).
10. (a) I. Fujii, N. Hiramaya, J. Ohtani, and K. Kodama, *Analytical Sciences* **12**, 153 (1996); (b) H. Schmidbaur, J. Lettenbauer, D. L. Wilkinson, G. Mueller, and O. Kumberger, *Z. Naturforschung. B* **46**, 901 (1991).

11. P. E. Burrows, Z. Shen, V. Bulovic, D. M. McCarty, S. R. Forrest, J. A. Cronin, and M. E. Thompson, "Relationship between Electroluminescence and Current Transport in Organic Heterojunction Light-Emitting Devices," *J. Appl. Phys.* **79**, 7991-8006 (1996).

12. A. Curioni and W. Andreoni, in preparation

13. Y. Hamada, T. Sano, M. Fujita, T. Fujii, Y. Nishio, and K. Shibata, *Jpn. J. Appl. Phys.* Pt. 2, **32**, L514 (1993). IP = 5.66 eV (UPS).

14. A. Schmidt, M. L. Anderson, and N. R. Armstrong, "Electronic States of Vapor Deposited Electron and Hole Transport Agents and Luminescent Materials for Light-Emitting Diodes," *J. Appl. Phys.* **78**, 5619-5625 (1995). IP = 5.93±0.1 eV (UPS).

15. M. Probst and R. Haight, "Unoccupied Molecular Orbital States of tris (8-hydroxy quinoline) Aluminum: Observation and Dynamics,"*Appl. Phys. Lett.* **71,** 202-204 (1997). IP = 6.0±0.1 eV (UPS).

16. A. Gavezzotti and G. Filipinni, "Energetic Aspects of Crystal Packing: Experiment and Computer Simulations," in *Theoretical Aspects and Computer Modeling of the Molecular Solid State*, Wiley, Chichester, 1997.

17. S. F. Alvarado, L. Libioulle, and P. F. Seidler, "STM-Excited Luminescence on Organic Materials," *Synth. Met.* **91**, 69-72 (1997); S. F. Alvarado, L. Rossi, P. Müller, P. F. Seidler, and W. Riess, "STM-Excited Electroluminescence and Spectroscopy on Organic Materials for Display Applications," this issue.

18. M. Brinkmann, G. Gadret, M. Muccini, C. Taliani, N. Masciocchi, and A. Sironi, "Correlation between Molecular Packing and Optical Properties in Different Crystalline Polymorphs and Amorphous Thin Films of *mer*-Tris(8-hydroxyquinoline)aluminum(III)," *J. Am. Chem. Soc.* **122**, 5147-5157 (2000).

19. P. Fernandez, A. Curioni and W. Andreoni, in preparation

20. A. C. Stueckl, C.A. Daul and H.U. Guedel, "Density Functional Calculations of Optical Excitation Energies by a Transition-State Method", *Int. J. Quantum Chem.* **61**, 579-588 (1997).

21. E. I. Haskal, private communication.

22. A. Curioni and W. Andreoni, "Material for Use in a Light Emitting Device and Highly Efficient Electroluminescence Device", European Patent application No. 99113398.4, filed July 12, 1999.

23. E. I. Haskal, A. Curioni, P. F. Seidler, and W. Andreoni, "Lithium-Aluminum Contacts for Organic Light-Emitting Devices," *Appl. Phys. Lett.* **71**, 1151-1153 (1997).

24. E. Tutis, M.-N. Bussac, L. Zuppiroli, "Image Force Effects at Contacts in Organic Light- Emitting Diodes", *Appl. Phys. Lett.* **75**, 3880-3882 (1999).

25. I. H. Campbell and D. L. Smith, "Schottky Energy Barriers and Charge Injection in Metal/Alq/Metal Structures", *Appl. Phys. Lett.* **74**, 561-563 (1999).

Table 1. Ionization potentials, electron affinities, extraction potentials and "small-polaron" stabilization energies for each isomer (in eV). See text for definitions. (v) and (a) indicate vertical and adiabatic values.

	IP(v)	IP(a)	HEP	SPE(h)	EA(v)	EA(a)	EEP	SPE(e)
facial	6.18	6.11	6.01	0.07	0.95	1.08	1.20	0.13
meridianal	6.15	6.11	5.99	0.04	0.94	1.00	1.13	0.06

Table 2. Binding energies (BE in kcal/mol) of the metal–Alq_3 complexes in the optimized configurations for both molecular isomers.

	Li	Al	Ca
facial	51	51	23
meridianal	39.5	37	11

Table 3. Ionization potentials and electron affinities of the metal–Alq_3 complexes (in eV). Definitions as in Table 1. Note that the values refer to the facial isomer of Alq_3.

	IP(v)	IP(a)	SPE(h)	EA(v)	EA(a)	SPE(e)
Li	3.85	3.79	0.06	0.85	0.9	0.06
Ca	4.01	3.95	0.06	1.09	1.12	0.03
Al	4.26	4.2	0.06	1.12	1.19	0.07

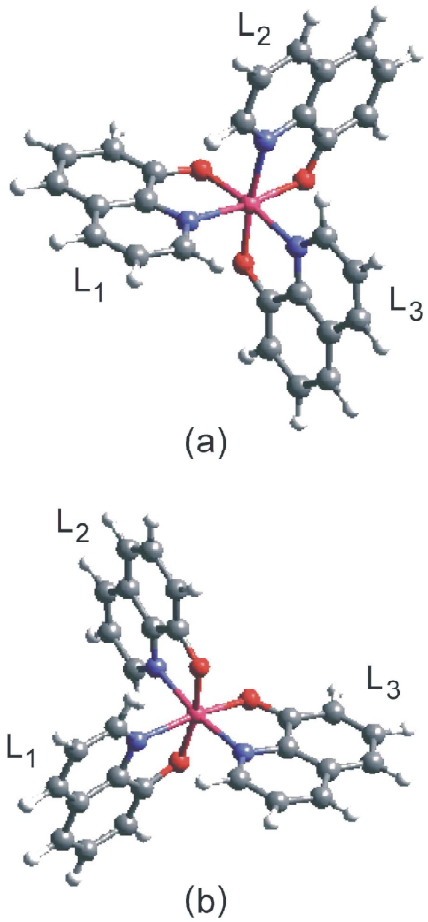

Figure 1. Structure of the two isomers: (a) facial and (b) meridianal. L_1, L_2, and L_3 denote the three ligands. Reprinted from [1], with permission from Elsevier Science.

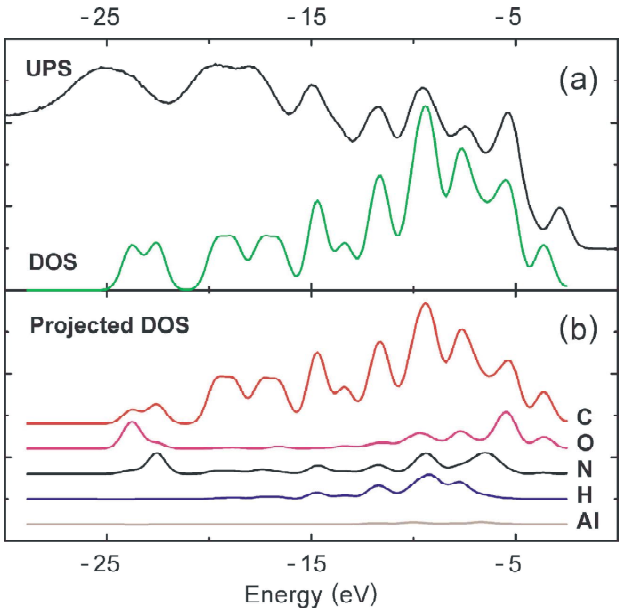

Figure 2. (a) Soft X-ray spectroscopy spectrum of Alq_3 and calculated-valence DOS. (b) Projected-valence DOS on the individual atomic species as labeled. Reprinted with permission from [2]. Copyright 1998 American Institute of Physics.

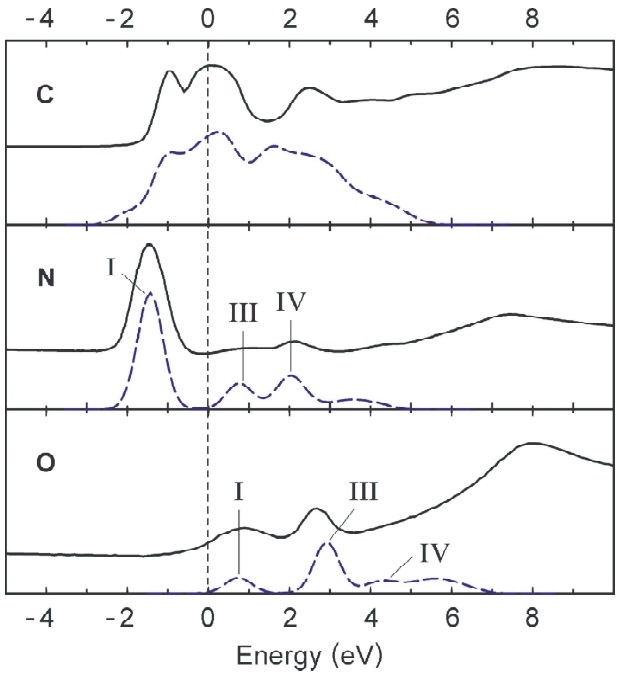

Figure 3. Comparison of 1*s* NEXAFS spectrum (solid curve) with calculated (dashed curve) photoabsorption for C, N, and O. The labels I–IV refer final states of the transition, namely to the LUMO (I), LUMO+1 (II), LUMO+2 (III) and LUMO+3 (IV) "triplets," respectively. Reprinted with permission from [2]. Copyright 1998 American Institute of Physics.

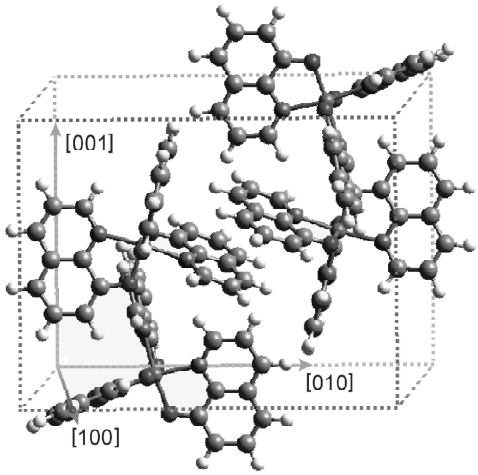

Figure 4. Crystal structure of Alq_3 according to Reference. 10b. Arrows indicate the direction of the reciprocal lattice basis vectors.

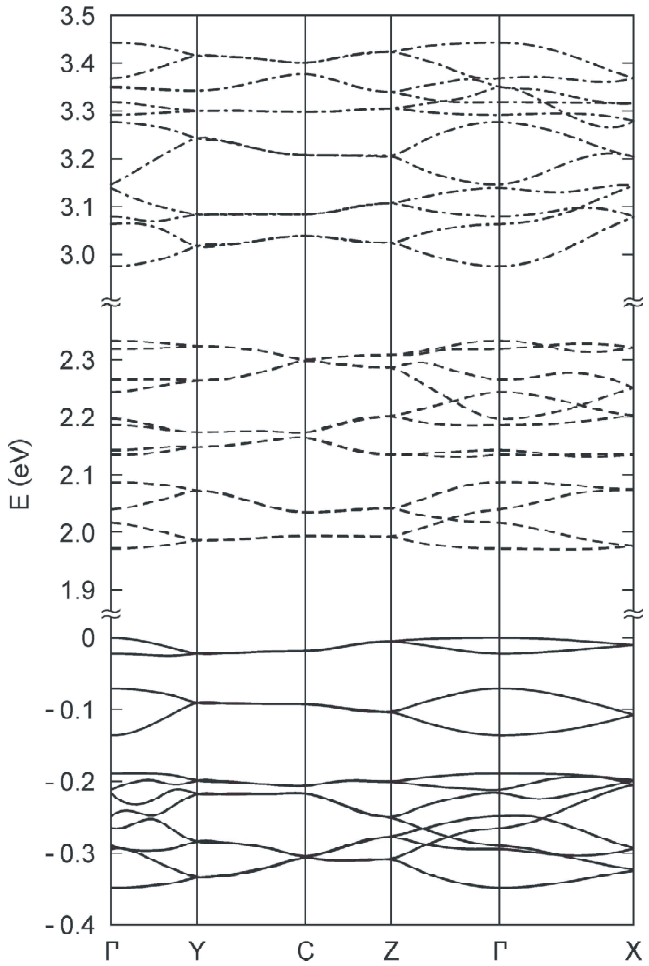

Figure 5. Electron energy bands of Alq_3 along some directions in the Brillouin zone. Γ = (0,0,0), Y = (0,½,0), C = (0,½,½), Z = (0,0,½), and X = (½,0,0), respectively, in units of the reciprocal lattice basis vectors.

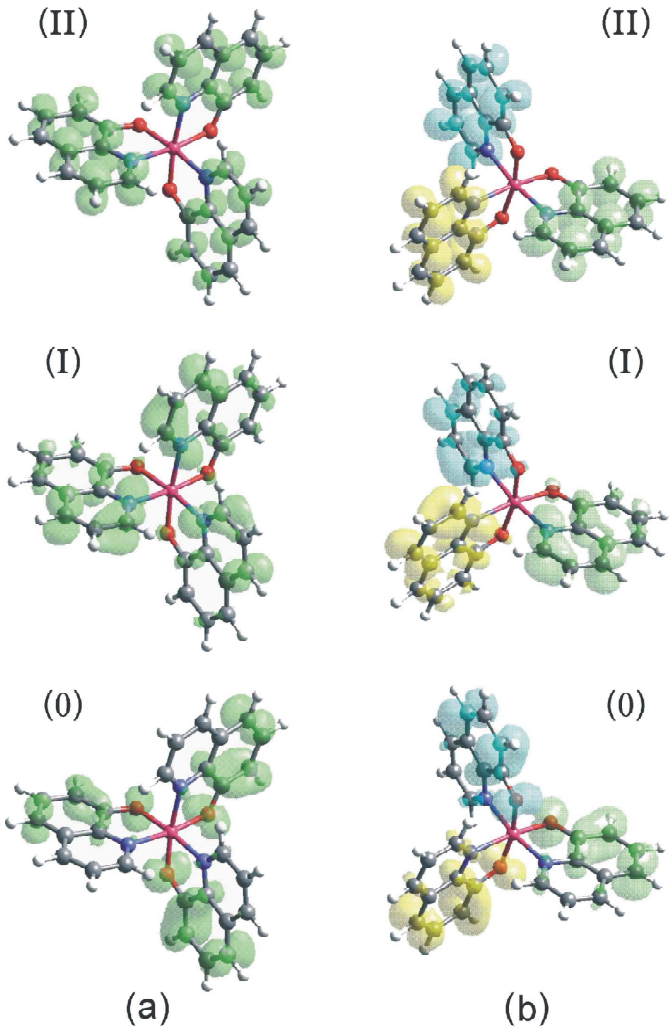

Figure 6. Isodensity surface of the distribution of the HOMO(0), LUMO(I), and LUMO+1(II) sets (a) in the facial isomer and (b) in the meridianal isomer. [0.001 e/(au)^3]. Reprinted from [1], with permission from Elsevier Science.

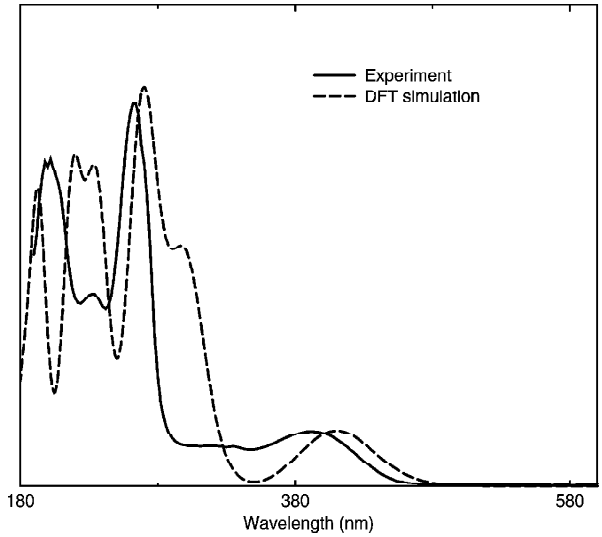

Figure 7. Calculated absorption spectrum of the meridianal molecular isomer of Alq_3 compared to experiment.

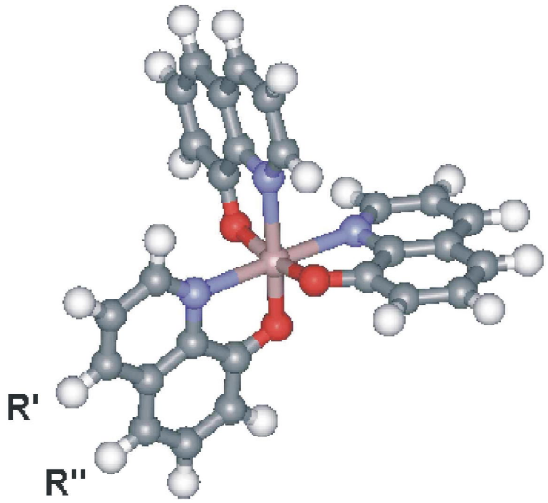

Figure 8. Structure of the newly proposed Alq_3 derivatives. Note that R′ = R″= H in Alq_3.

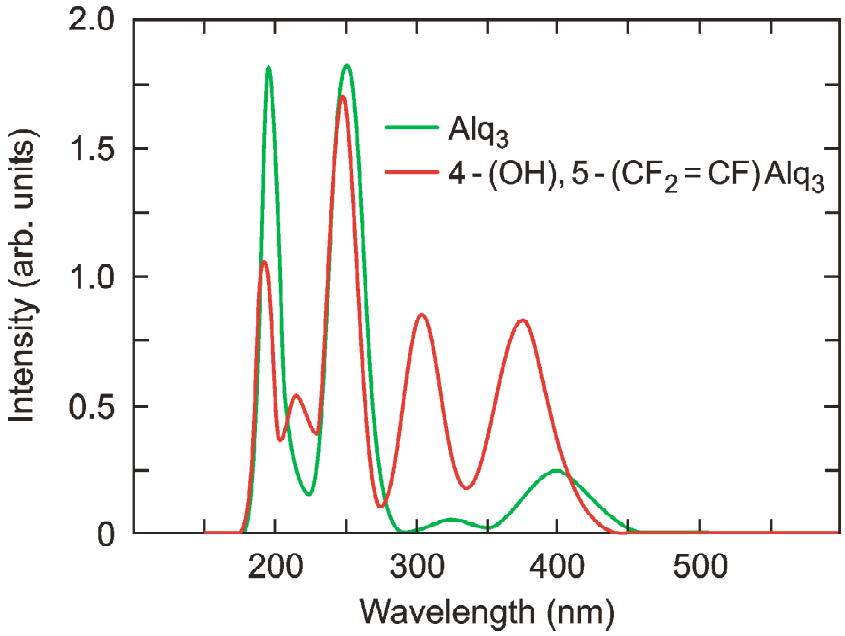

Figure 9. Calculated absorption spectrum of the specified Alq_3 derivative compared with that of Alq_3 (meridianal isomer).

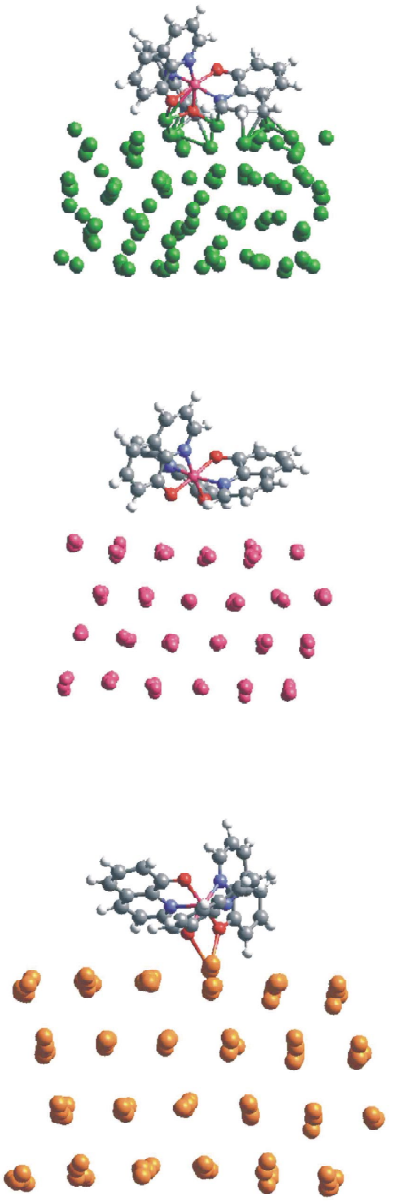

Figure 10. Snapshots of representative configurations from our molecular dynamics simulations of the interfaces of Alq_3 with (a) Li, (b) Al, and (c) Ca [(111) surfaces]. Reprinted from [4], with permission from Elsevier Science.

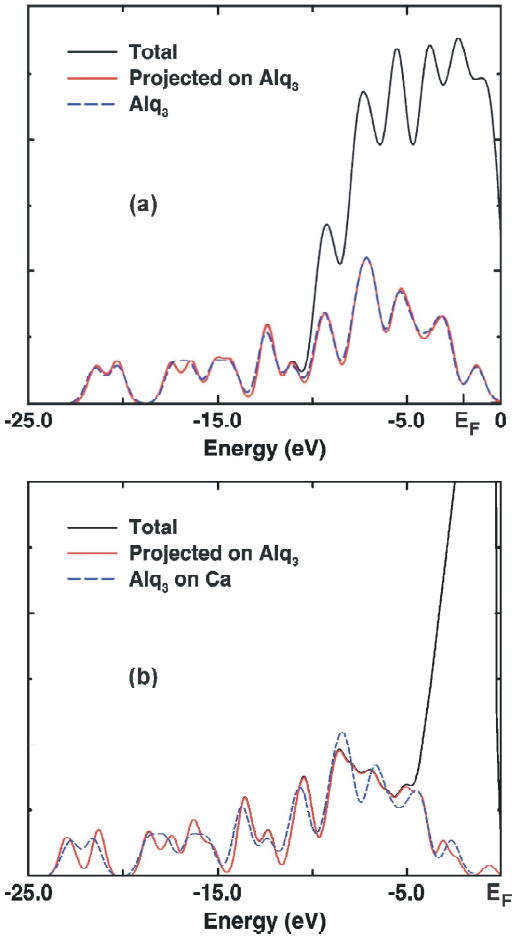

Figure 11. (a) Alq_3/Al(111) and (b) Alq_3/Ca(111) interfaces: calculated total DOS for the interface (solid black curve), projected on the molecule (solid red curve), and compared with that of the isolated molecule (dashed blue curve).

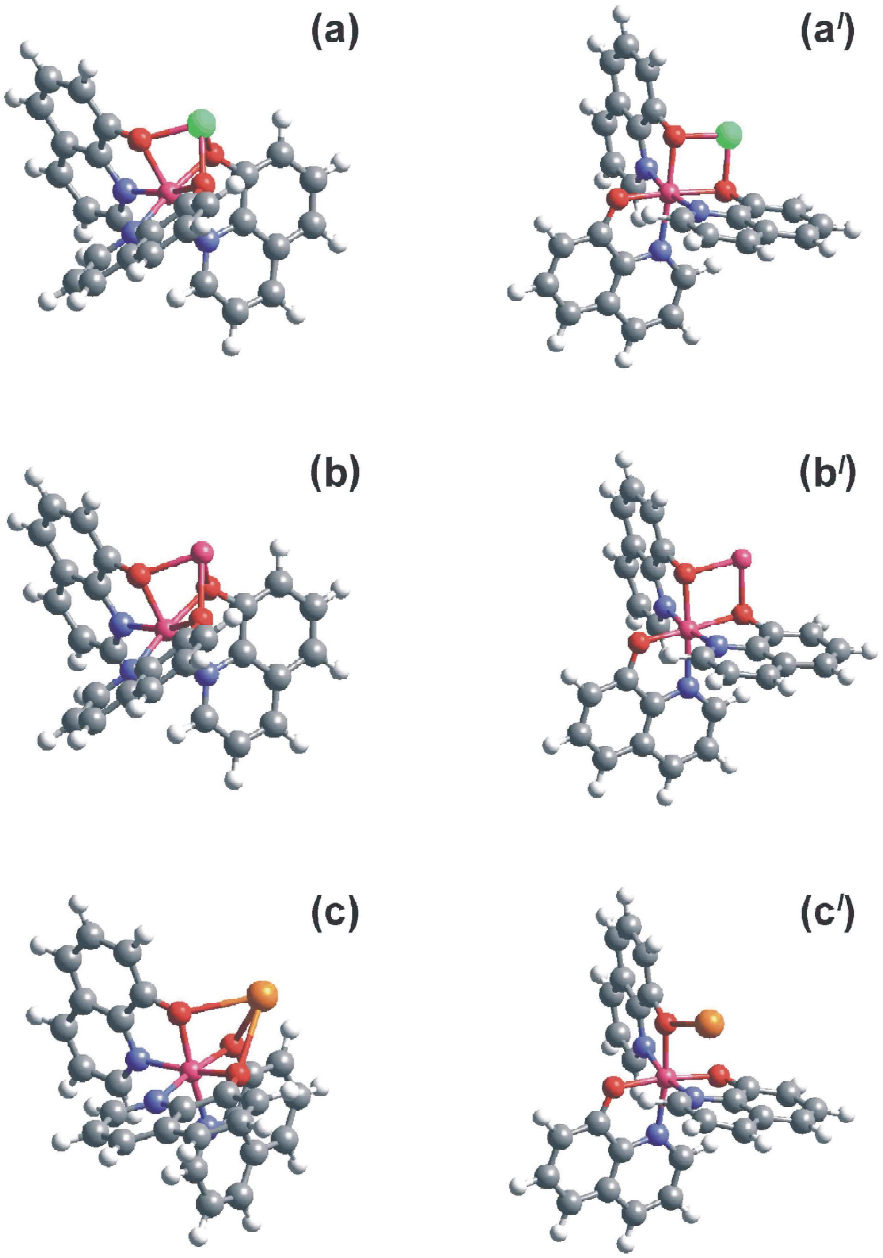

Figure 12. Minimum energy structures for (a) Li, (b) Al, and (c) Ca complexes with Alq_3 in the facial (left) and the meridianal (right) isomer. Reprinted with permission from [3]. Copyright 1999 American Chemical Society.